

COMPLEX INVESTIGATIONS IN DIAGNOSIS OF MAREK'S DISEASE IN POULTRY

Georgeta DINESCU, Elvira GAGNIUC, Gabriel TOMESCU

University of Agronomic Sciences and Veterinary Medicine of Bucharest, 59 Marasti Blvd,
District 1, Bucharest, Romania

Corresponding author email: elvira.gagniuc@fmvb.usamv.ro

Abstract

Marek's Disease is an oncogenic disease that affects both commercial and backyard poultry, caused by Alphaherpesvirus. Lymphoproliferative syndromes are characterized by lymphoma and are most commonly represented by T lymphocyte proliferation, with involvement of several visceral organs. Six poultry from the same population, aged between 1-12 years, non-vaccinated, have been examined after death. The following investigations have been done: gross examination, histopathology, immunohistochemistry (anti-CD3 antibody for T-lymphocytes and anti-PAX5 antibody for B-lymphocytes), and real-time polymerase chain reaction (RT-PCR). Macroscopically, all the poultry presented hepatic tumour nodules, along with tumoral enlargement of the sciatic nerve. Inconsistently, neoplasms in other organs, such as the spleen, heart, pharynx, and ovary, have been observed. The histopathological findings on the tumour mass showed a proliferation of small to large lymphocytes. Tumour cells were characterized by large pleomorphic nuclei with prominent nucleoli. The immunophenotype of transformed cells was identified as CD3 positive by immunohistochemistry; in contrast, PAX5 was negative. Virus presence confirmation was achieved through PCR. In conclusion, Marek's Disease can manifest in chronic form, at any age, being characterized by pleomorphic lymphocytic infiltration on a systemic involvement.

Key words: Marek's Disease, T lymphocytes, anti-CD3 antibody, systemic.

INTRODUCTION

Marek's Disease (MD) is a poultry contagious disease, with tumoral character, caused by *Gallid alphaherpesvirus 2* (GaHV-2), a DNA virus, from the *Mardivirus* genus, *Herpesviridae* family, *Alphaherpesvirinae* subfamily. It was first described in 1907 by the Hungarian veterinarian József Marek (Sharma & Sharma, 2020). It is an ubiquitous virus, resistant for long periods in the environment, especially in dust and shelters, since chickens spread the virus through their skin and feathers. There are three serotypes, the first of which has the highest virulence and oncogenic capacity. At present, there are only specific and nonspecific measures that can be taken against the disease, but no curative ones (Stiube, 2005; Boodhoo et al., 2016).

The infection is transmitted by the respiratory route, subsequently, the GaHV-2 is spread via a haematogenic way, infecting the lymphocytes. The virus replicates in the lymphoid line cells, attaching itself to their nucleus, and causing B cell cytolysis, simultaneously with activation of T lymphoid cells and reticulocyte hyperplasia.

Secondary, it is distributed on a systemic level; the main lesion is a consequence of T lymphocyte proliferation, which determines the pleomorphic infiltrate in tissues and organs, represented by lymphocytes in various differentiated cellular stages (Izumiya et al., 2019). Clinically, chickens present motor disorders, weakness, and high mortality (Graham, 2016; Brash et al., 2012).

This research had its starting point in the clinical suspicion of the disease in a poultry population grown in a household system, with ages between 1 and 12 years, in which a mortality rate of 90% was noted. The same manifestations of the disease have been noted in household systems from the same geographic area. The affected poultries had no contact with other birds and were not vaccinated or dewormed. Although in the affected households ducks were present, they did not manifest any symptoms, which strengthened the suspicion of a poultry infectious disease.

The study aims to present gross and microscopic lesions specific to GaHV-2 infection and to demonstrate the importance of modern methods

of investigation in establishing a certain diagnosis of Marek disease.

MATERIALS AND METHODS

Six birds were examined, a rooster and five hens, of common breed, with ages between 1 and 12 years of age. The region in which the cases were reported is the Neajlov riverbed, Giurgiu, Romania.

Establishing a diagnosis was in stages, ante-mortem and post-mortem, such as a clinical exam, necropsy, cytopathology and histopathological examination, immuno-histochemistry, and real-time polymerase chain reaction (RT-PCR).

The clinical exam aimed to evaluate constitution, behaviour, posture, exterior appearance, major clinical signs (digestive, respiratory, and nervous), and productivity (laying and fattening degree).

The necropsy focused on exterior appearance, with special attention being given to the feather follicle aspect. In opening the celomic cavity, the focus was aimed on the macroscopic appearance of the viscera. The examination continued with the skeletal muscle system, peripheral nervous system, and osteoarticular system (Dolz & Majo, 2019).

For cytopathology examination slides were prepared from the liver, spleen, gonads, and kidneys. The slides were prepared through scraping and smearing, stained with the May-Grünwald Giemsa method and examined with an optical microscope Olympus BX41. Samples of cutaneous tissue, brachial plexus and sciatic nerves, skeletal muscles, myocardium, lungs, spleen, kidneys, gonads, oviduct, liver, digestive system, cerebrum, cerebellum and eyes were sampled for histological examination. The samples were fixed in a 10% neutral buffer formalin solution, prepared following a paraffin embedding protocol, and routinely stained with haematoxylin-eosin (HE).

Additionally, in order to identify T or B cell markers of the tumour, immunohistochemical analysis (IHC) were performed on formalin-fixed, paraffin-embedded tissue, from nervous and liver tissue. We used CD3 (anti-CD3 (2GV6) Rabbit Monoclonal Primary Antibody) and an antibody against PAX5 (anti-PAX5 (SP34) Rabbit Monoclonal Primary Antibody)

that identify the T-lymphocytes (cytoplasmic region of the CD3 ϵ -chain) and B-lymphocytes (PAX-5 encodes for transcription factor B-cell-specific activator protein - BSAP). These antibodies were previously used by other authors (Stamilla et al., 2020) and proved cross-reactivity with chicken T- and B-lymphocytes. All histological and immunohistochemical slides were analysed using an Olympus BX41 microscope and digital micrographs were acquired using an Olympus DP25 digital camera.

For the PCR examination, samples of feathers, cloaca swabs (sterile swabs without medium), and nervous, genital, and lymph-hematopoietic tissue were sampled from case #4. Feathers were stored in a sterile container, and tissue samples (brain, ovary, and spleen) were fixed in 70% ethyl alcohol and preserved in tightly sealed sterile containers. The PCR test was performed in an external laboratory and the sample collection, fixation, and transport were done accordingly to the laboratory's recommendations.

RESULTS AND DISCUSSIONS

General clinical signs in the examined poultry were represented by lethargy, weight loss to emaciation, haemorrhagic diarrhoea, losses of equilibrium, paralysis, and death. The intensity of these manifestations was different for each individual, but the order of appearance was similar, spreading over a few weeks period. Firstly, progressive weight losses, without appetite alteration and with egg decrease, followed by progressive emaciation of the muscles and lethargy. Furthermore, cutaneous/subcutaneous proliferative changes have been noticed periocular, which determined an asymmetric deformation of the head (Figure 1). The final stages of the disease have shown nervous signs, such as abnormal vocalisations, loss of equilibrium, ataxia, incoordination, and abnormal positioning of wings and legs, followed by paralysis. The death occurred in a few days after instalment of nervous signs.

Exterior examination of the carcass, in the majority of cases (4/6), feathers were molted. The skin was scaled, especially in the pectoral and internal side of the legs area (Figure 2), and

the feather follicles presented hypertrophy, especially in the pectoral area (Figure 3). After skinning, a significant loss of subcutaneous conjunctive adipose tissue was observed, as well as generalized muscle atrophy, without noticing proliferative masses of tumoral lesions.



Figure 1. Periocular tumoral mass on the left side



Figure 2. Cachexia and severe skin scaling



Figure 3. Skin from the pectoral area, with hypertrophied feather follicle

It was aimed to bring forth the peripheral nervous plexus (brachial and sciatic) to identify the possible morphologic changes. These nervous structures inconstantly presented size

changes, with bilateral evolution, especially in the younger subjects (1-2 years of age). Macroscopically, the enlarged growth was noticed, with matting and grey-yellow colour (Figures 4 and 5).



Figure 4. Left leg. Sciatic nerve with enlarged growth, matted and of grey-yellow colour



Figure 5. Left-wing. Brachial plexus - enlarged, matted, grey-yellow colour

The cerebrum, cerebellum, and brain stem were eviscerated as one piece (Figure 6) and were examined on the surface as well as in the section; no gross lesions were identified.



Figure 6. Cerebral tissue on a longitudinal section

In all cases examined, the liver resented hepatomegaly and on the visceral side and free margins of the lobes white, fatty, compact in-section nodules were observed (Figure 7).



Figure 7. Liver. Multifocal white proliferations

In cytology examination, abnormal morphologic changes were observed only in the slides from the liver at hepatocytes cells, expressed by intracytoplasmic vacuolization, erythrocytes, and moderate number of tumoral cells - lymphoblasts (Figure 8). In all other slides, no observed the malignant lymphoid cells.

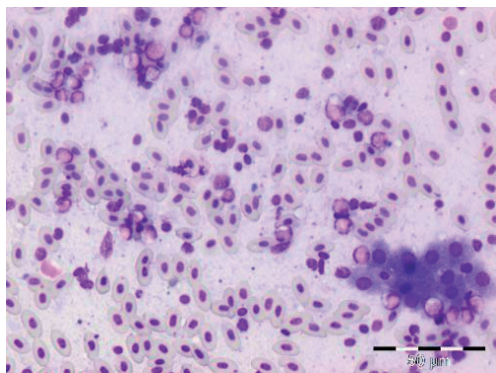


Figure 8. Liver cytology. Hepatocytes with intracytoplasmic vacuolization, erythrocytes, and a moderate number of tumoral lymphoblasts (x400, MGG)

At cutaneous tissue, we observed changes in dermal architecture and feather follicles with a pleomorphic lymphocytic infiltrate, disposed of diffuse or nodular. In the *dermal papillae*, a severe lymphocytic infiltrate can be observed. Different structures of the feather follicle can't be differentiated (*dermal papillae*, pulp,

stratum germinativum, and *epidermal collar*) (Bacha & Bacha, 2012), and follicular *stratum corneum* and the muscle fibres of the feather follicle appear hypertrophic/hyperplasic (Figure 9). Furthermore, barbs stems appear infiltrated with pleomorphic lymphocytes (Figure 10).



Figure 9. Feather follicle with altered histologic structure, only the follicular *stratum corneum* can be differentiated. Abundant pleomorphic lymphocytic infiltrates the *dermal papillae* and pulp, also hypertrophy of follicular muscle fibres (x200, HE)

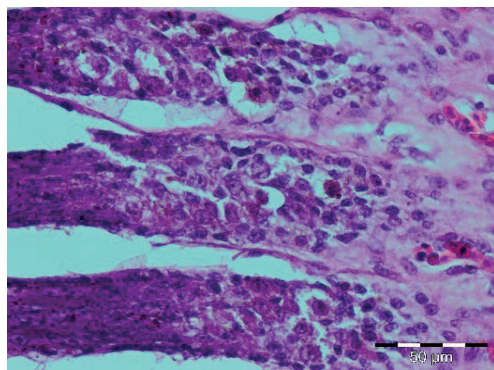


Figure 10. Barbs stems with tumoral lymphocyte pleomorphic infiltrate (x400, HE)

In peripheral nervous tissues, on histopathologic examination, we observed dilacerations of the nerve fibres with oedema can be observed of abundant pleomorphic tumoral lymphocytic infiltrate. Also, the cellular infiltrate was found in perivascular cuffing appearance, as well as diffuse infiltrate (Figure 11).

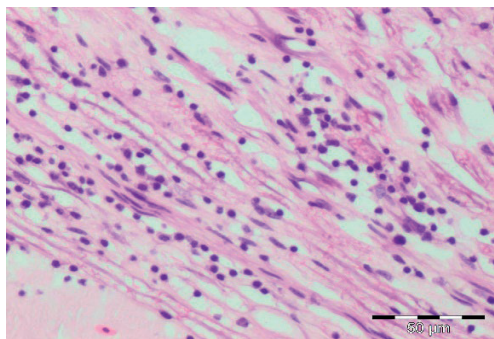


Figure 11. Peripheral nerve, longitudinal section. Mononuclear infiltrate that dilacerates the nervous fibres (x400, HE)

In the skeletal muscles (Figures 12 and 13) similar lesions to those described in the nervous tissue have been found, noticeable being the severe dilacerations of the muscle fibres, perivascular cuffing, and diffuse appearance of the pleomorphic lymphocytic infiltrate, as well as the necrosis of the muscle cells.

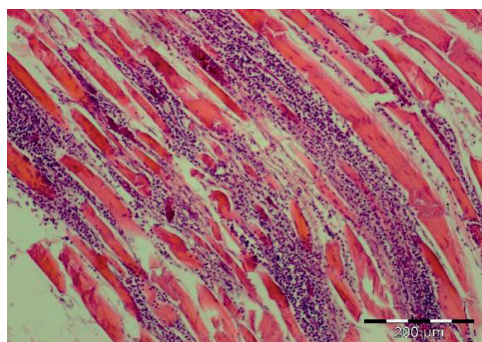


Figure 12. Skeletal muscle, longitudinal section. Abundant pleomorphic lymphocytic infiltrate, with severe dilacerations of the muscle fibres and oedema (x100, HE)

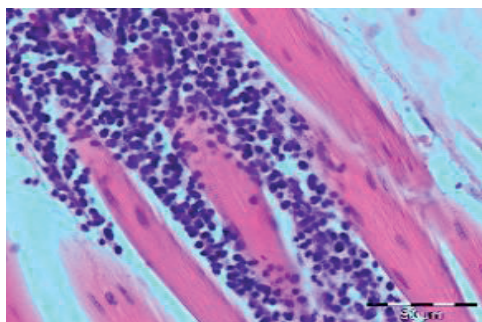


Figure 13. Skeletal muscle, longitudinal section. Pleomorphic lymphocytic infiltrate disposed of diffuse, with muscle fibre necrosis (x400, HE)

Histopathologic examination of the cerebellum brought forth the presence of tumoral infiltrate in its layers - molecular, Purkinje neurons, and granular (Figure 14).

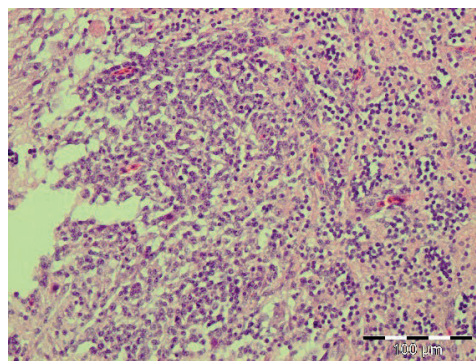


Figure 14. Cerebellum. Microscopic lesion of tumour mass, the uniform proliferation of tumoral lymphoblast and small to medium lymphocyte (x200, HE)

A perineuronal oedema can be observed, as well as pleomorphic lymphocytic infiltrate disposed of diffuse or perivascular and perineuronal cuffing. The Purkinje cells layer is marked by neuronal necrosis and satellitosis, from place to place the Purkinje cells are replaced by neoplastic cells (Figure 15). These histologic aspects explain the severity and evolution of the neurological clinical signs in the late stages of the disease.

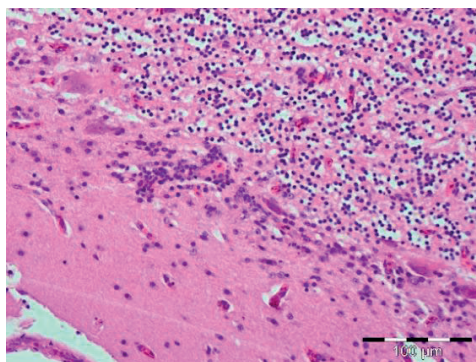


Figure 15. Cerebellum. Severe pleomorphic lymphocytes infiltration of the Purkinje layer with neuronal necrosis, satellitosis and perivascular cuffing (x200, HE)

The pleomorphic lymphocytic infiltrate presented the highest degree of proliferation in the central nervous tissue, with lesions being extended, and extremely severe (Figures 16 and 17).

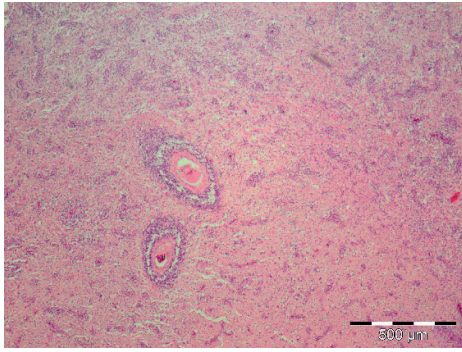


Figure 16. Cerebrum. Overview, neuropil with diffuse pleomorphic lymphocytic infiltrate and perivascular cuffing and oedema (x40, HE)

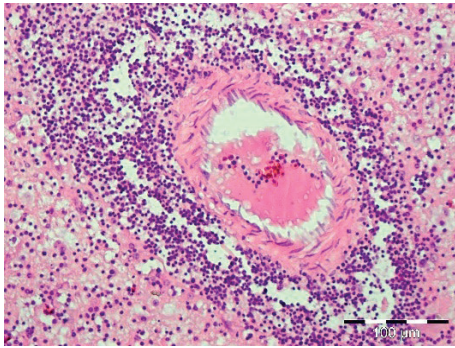


Figure 17. Cerebrum. Arterial wall with severe infiltrate in the *tunica adventitia*. Lymphocytic population with extension tendency in the neuropil, generating perivascular oedema (x200, HE)

In the cerebrum, the same changes have been noticed, expressed by severe perivascular cellular infiltrate associated with oedema in the Virchow-Robin space. Furthermore, neuronal necrosis, gliosis, and satellitosis can be identified (Figure 18).

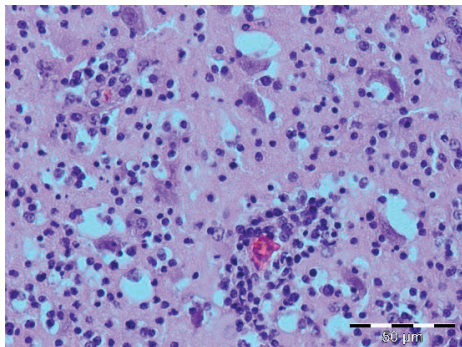


Figure 18. Cerebrum. Pleomorphic lymphoblasts, oedema in the Virchow-Robin space, satellitosis, and gliosis (x400, HE)

Severe histopathologic lesions were found in the liver, with the destruction of the vascular parietal structure due to the abundant presence of the pleomorphic lymphocytic population. The same tumoral infiltrate was observed around bile ducts, but also in their lumen (Figure 19). Neoplastic cells infiltrated Disse spaces, causing oedema (Figure 20). Histopathological examination of the other viscera (myocardium, lungs, spleen, kidneys, gonads, oviduct, digestive system) revealed similar aspects as those described in the liver.

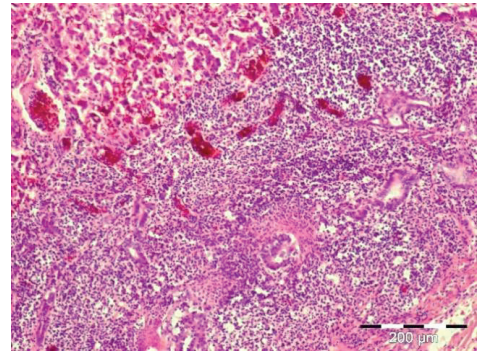


Figure 19. Liver. Diffuse pleomorphic lymphocytic infiltrate in the hepatic parenchyma, with the destruction of tissue architecture. Hepatocytes necrosis can be observed, congestion and bile ducts surrounded by neoplastic cells (x100, HE)

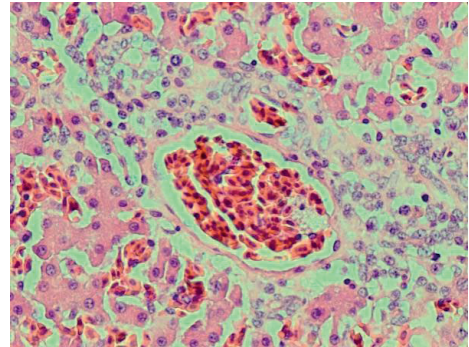


Figure 20. Liver. Tumoral cells re-infiltrated around the centrilobular veins and Disse spaces (x400, HE)

The Cluster Differentiation 3 (CD3) is a protein complex and T cell co-receptor that is involved in activating both the cytotoxic T cell (CD8+ native T cell) and T helper cells (CD4+ native T cells). In the samples, most of these cells resulted in CD3 stained in a form of membrane precipitate, brown coloured in the IHC analysis, as reported in Figures 21 and 22.

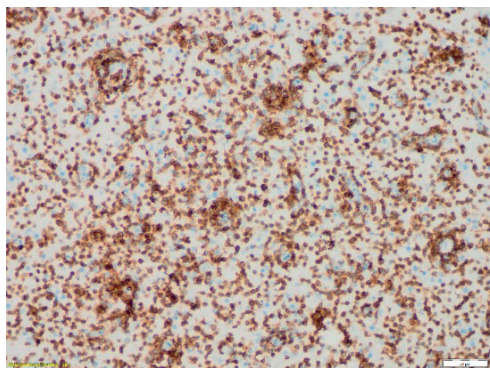


Figure 21. Cerebrum. IHC CD3, diffuse positive staining (x200)

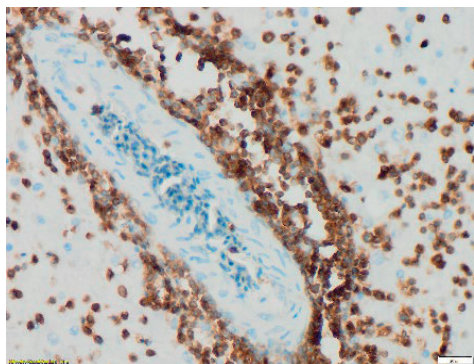


Figure 22. Cerebrum. Blood vessel CD3, diffuse positive staining (x400)

The immunophenotype of transformed cells was identified as CD3 positive by immunohistochemistry; in contrast, PAX5 (B cell marker) was negative.

The T lymphocytes in the liver were marked positive for anti-CD3 antibodies, confirming the tumoral cells population (Figure 23).

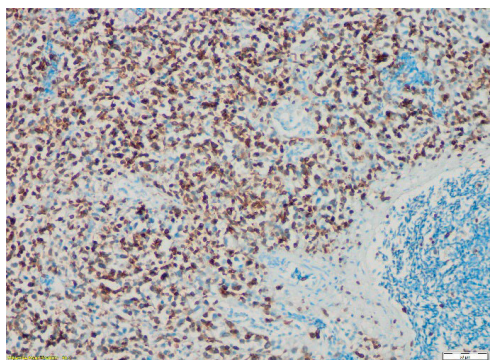


Figure 23. Liver. IHC CD3, diffuse positive staining (x200)

The present study highlights the importance of complex investigation in establishing a diagnosis of Marek's Disease. This subject was less approached nationally in the last years; the last study conducted presented the evolution of an outbreak of Marek's in broiler chickens and in layer youth raised in an intensive system in western Romania (Fodor et al., 2009).

The present study reports for the first time the presence of GaHV-2 naturally infected layer adults of different ages (1-12 years), raised in the household system, in Romania. Thus, comparison of the results of this study with those of other recent existing studies is limited for this age category. In the study above mentioned (Fodor et al., 2009), disease evolution was acute, and there were no macroscopic changes noted in the nerves, viscera, and skin, but histologic findings were similar to those described in our study, respectively the presence of a pleomorphic lymphocytic population, appearance diffuse or perivascular cuffing in different tissues and organs.

A few international scientific studies (Mete et al., 2016; Dunn et al., 2020; Abreu et al., 2016) described the disease evolution in chickens with ages up to 3 years, but in this study, one of the subjects was 12 years old. Since in the Romanian household system, it is rare to find chickens above 5 years of age, we consider that bringing forth the fact that GaHV-2 infection and specific lesions in poultry over 10 years represent a novelty of this paper. Even though the histopathological findings described are similar to those exposed in other scientific papers (Das et al, 2018; Dunn et al., 2020; Abdul-Aziz et al., 2016; Suma et al., 2018), the present study shows the existence of microscopic lesions specific for MD constantly, in all examined subjects.

Currently, confirmation of the disease through IHC and RT-PCR is constantly used (Stamilla et al., 2020; Wilson et al., 2022; Mete et al., 2016).

The complex investigations in this study allowed the differential diagnosis compared to other morbid entities in which MD can be confused.

CONCLUSIONS

General clinical signs in the subjects examined were unspecific: lethargy, weight loss to emaciation, haemorrhagic diarrhoea, equilibrium loss, paralysis, and death, aspects that can be encountered in various poultry diseases.

Results of gross and microscopic examinations described a complex overview of Marek Disease, expressed by infiltration of a pleomorphic lymphocytic population in the skin, central and peripheral nervous system, skeletal muscle tissue, and liver.

Infiltration of T tumoral lymphocytes in cutaneous tissue and feather follicles is specific to the diseases once the dust generated by skin scaling and feathers from infected poultry are virus reservoirs.

Oedema associated with the pleomorphic lymphocytic perivascular infiltrate and cellular necrosis in the skeletal muscle system and nervous system explains the neuromotor clinical signs of the disease.

Positive response in immunophenotyping cells with CD3 allowed the highlighting of T lymphocytes specific to MD proliferation. Confirming Marek's disease diagnosis, by identifying the virus, was done through RT-PCR.

REFERENCES

- Abdul-Aziz, T., Barnes, H., Fletcher, O., & Swayne, D. (2016). Nervous System. In T. Abdul-Aziz, H. Barnes, & O. Fletcher, *Avian Histopathology Fourth Edition* (pp. 469-519). Florida, USA: The American Association of Avian Pathologists, Inc.
- Abreu, D., Santos, F., Jose, D., Tortelly, R., Pereira, V., & Nascimento, E. (2016). Pathological Aspects of a Subclinical Marek's Disease. Case in Free-Range Chickens. *Brasilian Journal of Poultry Science*, 198.
- Bacha, L., & Bacha, W. (2012). *Color Atlas of Veterinary Histology Third Edition*. Chichester, UK: John Wiley & Sons, Inc.
- Boodhoo, N., Gurug, A., Sharif, S., & Behboudi, S. (2016). Marek's disease in chickens: a review with focus on immunology. *BioMed Central*, 1-2. doi:10.1186/s13567-016-0404-3
- Brash, M., Ojkic, M., & Shivaprasad, H. (2012). Viral Diseases. In M. Boulianne, *Avian Disease Manual* (pp. 30-31). Florida, USA: The American Association of Avian Pathologists, Inc.
- Das, S., Das, D., Panda, S. K., Sagarika, S., & Jena, B. (2018). Clinico-Pathological Studies of Marek's Disease in Chickens. *International Journal of Livestock Research*, 8, 207-217.
- Dolz, R., & Majo, N. (2019). *Atlas of Avian Necropsy, Macroscopic Diagnosis Sampling*. Zaragoza, Spain: Grupo Asis Biomeda, SL.
- Dunn, J., Gimeo, I., & Nair, V. (2020). Marek's Disease. In D. Swayne, *Diseases of Poultry, 14th Edition* (pp. 562-564). Hoboken, USA: John Wiley & Sons, Inc.
- Fodor, I., Coman, M., & Catana, N. (2009). An Outbreak of Marek's Disease in Broiler Chickens: Epidemiological, Clinical and Anatomopathological Aspects. *Lucrari Stiintifice Medicina Veterinara, XLII (1)*:1-4. Timisoara: Faculty of Veterinary Medicine Timisoara.
- Graham, J. (2016). Viral Neoplasms: MD, LL and RE. In J. Graham, *Blackwell's Five -Minute Veterinary Consult, Avian* (pp. 302-304). Massachusetts, USA: John Wiley & Sons, Inc.
- Izumiya, Y., Jin, D., Lupiani, B., Liao, Y., & Reddy, S. (2019). Marek's Disease Virus. In S. Samal, *Avian Virology, Current Research and Future Trends* (pp. 345-364). Norfolk, UK: Caister Academic Press.
- Mete, A., Gharpure, R., Piresky, M., Famini, D., Sverlow, K., & Dunn, J. (2016). Marek's Disease in Backyard Chickens, A Study of Pathologic Findings and Viral Loads in Tumorous and Nontumorous Birds. *Avian Diseases*, 60, 826-836.
- Sharma, R., & Sharma, N. (2020). Marek's Disease. In N. Sharma, & R. Sharma, *Avian Pathology, A Colour Handbook* (pp. 159-165). New Delhi, India: New India Publishing Agency.
- Stamilla, A., Messina, A., Condorelli, L., Licitra, F., Antoci, F., Lanza, M., . Puleio, R. (2020). Morphological and Immunohistochemical Examination of Lymphoproliferative Lesions Caused by Marek's Disease Virus in Breeder Chickens. *Animals: an open acces journal from MDPI*, 10(8), 1280.
- Stiube, P. (2005). Boala lui Marek. In R. Manzat, *Boli Virolice si Prionice ale Animalelor* (pp. 106-166). Timisoara, Romania: Brumar.
- Suma, U., Rahman, M., Nooruzzman, M., Chowdhury, E. H., & Islam, M. R. (2018, december). Pathology of Marek's disease in layer chickens in Bangladesh. *Bangladesh Veterinarian*, 34(2):35-41. doi:10.3329/bvet.v34i2.49886
- Wilson, L., Lewis, M., Baigent, S., Abate, V., Dolega, B., Morrison, L., Walker, D. (2022). Marek's Disease in an Indian Peafowl (*Pavo cristatus*) with Clinical Ocular Disease and Paraparesis. *Journal of Comparative Pathology*, 195, 7-11.